INSTITUTE OF PHYSICS PUBLISHING JOURNAL OF OPTICS A: PURE AND APPLIED OPTICS

J. Opt. A: Pure Appl. Opt. **6** (2004) 36–42 PII: S1464-4258(04)63543-4

Bayesian pattern recognition in optically degraded noisy images

Rafael Navarro, Oscar Nestares and Jose J Valles

Instituto de Óptica 'Daza de Valdés', Consejo Superior de Investigaciones Científicas, Serrano 121, 28006 Madrid, Spain

Received 15 May 2003, accepted for publication 8 September 2003
Published 24 September 2003
Online at stacks.iop.org/JOptA/6/36 (DOI: 10.1088/1464-4258/6/1/008)

Abstract
We present a novel Bayesian method for pattern recognition in images affected by unknown optical degradations and additive noise. The method is based on a multiscale/multiorientation subband decomposition of both the matched filter (original object) and the degraded images. Using this image representation within the Bayesian framework, it is possible to make a coarse estimation of the unknown optical transfer function, which strongly simplifies the Bayesian estimation of the original pattern that most probably generated the observed image. The method has been implemented and compared to other previous methods through a realistic simulation. The images are degraded by different levels of both random (atmospheric turbulence) and deterministic (defocus) optical aberrations, as well as additive white Gaussian noise. The Bayesian method proved to be highly robust to both optical blur and noise, providing rates of correct responses significantly better than previous methods.

Keywords: pattern recognition, optical degradations, Bayesian OTF estimation, atmospheric turbulence, image processing

1. Introduction

Pattern recognition is an extremely useful technique in image analysis, spanning a large variety of applications [1], from object recognition to image retrieving and classification. Traditional pattern recognition methods, based on matching or correlation, are highly attractive, but their main drawback is that they are strongly sensitive to optical degradations and noise in the observed images. There is a large number of references in the literature proposing correlation-based pattern recognition methods to obtain invariant pattern recognition against different transformations, distortions and all kinds of degradation of the image [2]. Many studies have focused on geometric distortions, such as scaling and rotation [3–5], and also on pattern recognition or localization in the presence of noise [6–10]. Less work has been done in optically degraded images [11], where most of the published works deal with the particular case of defocus [12, 13]. There is however a lack of methods able to deal robustly with images doubly degraded by the combined effect of optical aberrations (or scattering) and noise.

In this work, we propose and test a novel Bayesian approach, for pattern recognition robust to the combined effect of optical degradations (aberrations, etc) and noise on the image. The Bayesian approach consists of a probabilistic formulation, classic in many estimation or decision-making problems, which has also been used in pattern recognition [9]. In a previous publication, Vargas *et al* [13] obtained invariant pattern recognition against defocus by first applying a subband decomposition of the matched filter, and then combining the correlation outputs of each channel in a multiplicative way. This proved to be a highly efficient method to remove potential false alarms, which otherwise would soon appear with defocus. Based on that work, we have generalized the method, by introducing a probabilistic Bayesian framework that permits us to deal with a more general form for the optical degradation (modelled as an optical transfer function (OTF) linear filter) and to include additive noise. Here, we make use of a subband decomposition, but instead of the multiscale Laplacian pyramid [14] used in [13] to deal with pure defocus, here we apply a multiscale/multiorientation Gabor pyramid [15], which permits us to deal with more general non-symmetric optical degradations.

There are situations where optical degradations are constant or can be calibrated somehow, so that this *a priori* knowledge can be available to the recognition algorithm.

However, in the present study, we are interested in the cases where the optical degradation is unknown, such as image degradations introduced by random or unpredictable motion, atmospheric turbulence, or turbid media in general. The proposed Bayesian method implicitly estimates a coarse approximation of the OTF to find the pattern that most probably generated the observed image.

To test the different methods, including the one proposed here, we have carried out a realistic simulation where the task was to classify flying birds (different eagles and falcons species) observed through a telescope in the presence of atmospheric turbulence. The images were also affected by additive Gaussian noise. Our method, which compares favourably with other previous approaches, provided high recognition rates even for large optical degradations and low signal to noise ratios.

2. Methods

The Bayesian method consists of three main elements:

(1) an observation model consisting of linear filtering of the object with the OTF and additive noise;
(2) a multiscale/multiorientation decomposition of the image giving rise to a set of observed subbands; and
(3) a Bayesian framework to estimate the pattern that most probably generated the observed image, as well as a coarsely sampled estimate of the OTF.

The optical degradation is modelled as a generic complex low-pass linear filter. Its modulus, the modulation transfer function (MTF), causes contrast attenuation to the different spatial frequencies in the object, while the phase transfer function (PTF) produces a different shift to each spatial frequency. The proposed method explicitly assumes that the OTF is unknown, and the strategy is to implicitly estimate the OTF during the recognition process. The blur in the image domain is given by the point spread function (PSF) that is the Fourier transform of the OTF.

Therefore, we have to consider that, for an optimal recognition performance, we have to simultaneously estimate two unknowns, the original pattern and the OTF. The main problem with this general approach is that it is not well constrained, and therefore to solve this double estimation (or recognition) problem we need to include some *a priori* information, which is straightforward in the Bayesian framework.

Using *a priori* knowledge, we can make approximations that permit us to constrain the recognition problem. First we apply a most usual constraint, based on the assumption that the object belongs to a finite set of possible objects. For instance, in character recognition, the object belongs to the alphabet. Regarding the second unknown, we also propose to strongly constrain the space of possible degradations (or OTFs). To this aim, we introduce the subband decomposition of the image, by applying a bank of multiscale band-pass filters tuned to different spatial frequencies and orientations. This type of image decomposition provides a number of subbands, which can be realized as a discrete coarse sampling of the frequency domain [16]. Then, the key idea is to apply the same coarse sampling to the OTF. This permits us to make a strong simplification that is to assume that the OTF is constant within each subband. This limits greatly the space of possible OTFs, which can be approximated by a multiplicative constant and a linear phase inside each subband. In our case, we apply a multiscale/multiorientation Gabor decomposition [15], which yields a log-polar sampling of the frequency domain, which has proved to be highly convenient in many applications [16], and has been described in [17], including implementation details. In particular, this sampling is well adapted to typical OTFs, which tend to change more steeply in the low-frequency range and become shallower as the frequency increases.

However, such a coarse sampling cannot follow rapidly varying OTFs, such as the undulating OTF produced by a strong defocus, then providing a false (aliased) representation of this type of degradation. Thus the method could fail for large degradations, mainly for those presenting complicated or wavy patterns in the OTF. This will be, in fact, its main limitation, since it is guaranteed to work properly only when the approximation of constant OTF within each subband holds reasonably well, that is with moderate optical degradations producing a smooth enough OTF. Nevertheless, the practical performance and limitations of this method will be assessed empirically in section 4.

Putting these ideas together, let us formulate the observation model for the ith band-pass filtered version of the image $o_i(\mathbf{x})$. According to this model, the observed image $o_i(\mathbf{x})$ is the result of applying the ith filter $g_i(\mathbf{x})$ to the image. The image itself is the convolution of the original pattern $f(\mathbf{x})$ with the impulse response of the unknown optical degradation, $h(\mathbf{x})$, plus noise, $\eta_i(\mathbf{x})$ (here the noise is band-pass since it has also been convolved by filter $g_i(\mathbf{x})$):

$$o_i(\mathbf{x}) = (h(\mathbf{x}) * f(\mathbf{x})) * g_i(\mathbf{x}) + \eta_i(\mathbf{x}), \quad i = 1, \ldots, N_c \quad (1)$$

where N_c is the number of channels, and $*$ means spatial convolution.

Now, we make use of the main approximation as described before, namely the OTF is constant within a channel (or subband). Its effect upon the observed subband image is a modulation h_i plus a global shift $\mathbf{u}_i$:

$$o_i(\mathbf{x}) \approx h_i f_i(\mathbf{x} - \mathbf{u}_i) + \eta_i(\mathbf{x}), \qquad i = 1, \ldots, N_c \quad (2)$$

where $f_i(\mathbf{x}) = f(\mathbf{x}) * g_i(\mathbf{x})$ is the ith subband of the original pattern, that is filtered with the ith bandpass channel. The parameters $(h_i, \mathbf{u}_i)$ are, respectively, the modulation factor and the global shift approximating the optical degradation within the bandwidth of the ith filter. Ideally, one would need to estimate $(h_i, \mathbf{u}_i)$ for a continuum of spatial frequencies, but this would make the mathematical problem ill posed. Our approach is equivalent to applying a coarse sampling of the OTF in the frequency domain. The coarseness or smoothness of the sampling would depend on the number of channels (subbands) used.

Given this strongly simplified observation model, we can now formulate the joint posterior probability for the original input pattern $\mathbf{f}$, and for the approximated linear degradation model parameters $\{h_i, \mathbf{u}_i\}$. Given the observations $\{\mathbf{o}_i\}$ and applying Bayes' rule we obtain

$$p(\mathbf{f}, \{h_i, \mathbf{u}_i\} | \{\mathbf{o}_i\}) = K p(\{\mathbf{o}_i\} | \mathbf{f}, \{h_i, \mathbf{u}_i\}) p(\mathbf{f}) p(\{h_i, \mathbf{u}_i\}) \quad (3)$$

where, for notational convenience, we have expressed images as intensity vectors; K is a normalization constant. The posterior probability is proportional to the likelihood (or conditional probability of the observations, given the input pattern and the degradation parameters) multiplied by the prior probability. In the previous expression we have assumed that the input pattern $\mathbf{f}$ is statistically independent of the linear degradation model parameters $\{h_i, \mathbf{u}_i\}$. If we further assume a constant prior probability for the degradation parameters $\{h_i, \mathbf{u}_i\}$, then the posterior probability is finally

$$p(\mathbf{f}, \{h_i, \mathbf{u}_i\}|\{\mathbf{o}_i\}) = K' p(\{\mathbf{o}_i\}|\mathbf{f}, \{h_i, \mathbf{u}_i\}) p(\mathbf{f}) \tag{4}$$

where K' is another normalization constant. The maximum *a posteriori* (MAP) estimator for the input pattern $\hat{\mathbf{f}}$ and for the linear degradation parameters $\{\hat{h}_i, \hat{\mathbf{u}}_i\}$ is the one that maximizes the posterior probability in equation (4):

$$(\hat{\mathbf{f}}, \{\hat{h}_i, \hat{\mathbf{u}}_i\}) = \underset{(\mathbf{f}, \{h_i, \mathbf{u}_i\})}{\arg\max}\, p(\{\mathbf{o}_i\}|\mathbf{f}, \{h_i, \mathbf{u}_i\}) p(\mathbf{f}) \tag{5}$$

where the likelihood function $p(\{\mathbf{o}_i\}|\mathbf{f}, \{h_i, \mathbf{u}_i\})$ is given by the probability density function of the noise p_{η_i}, according to the observation model in equation (2). If we further assume conditional independence between channels and between spatial locations inside the channels, the likelihood is then given by

$$p(\{\mathbf{o}_i\}|\mathbf{f}, \{h_i, \mathbf{u}_i\}) = \prod_{i=1}^{N_c} \prod_{\mathbf{x}} p_{\eta_i}(o_i(\mathbf{x}) - h_i f_i(\mathbf{x} - \mathbf{u}_i)). \tag{6}$$

Now, we can incorporate all the *a priori* information as a prior probability on the input image $\mathbf{f}$. From the assumptions of the recognition problem, we know that the input image belongs to a finite set $\{\mathbf{f}^j\}_{j=1}^N$, where N is the total number of patterns. The assumption of having a limited set of possible patterns heavily constrains the space of all the possible intensity configurations of the input image, resulting in a posterior probability that is different from zero only when $\mathbf{f} \in \{\mathbf{f}^j\}_{j=1}^N$:

$$p(\mathbf{f} = \mathbf{f}^j, \{h_i, \mathbf{u}_i\}|\{\mathbf{o}_i\}) \propto \prod_{i=1}^{N_c} \prod_{\mathbf{x}} p_{\eta_i}(o_i(\mathbf{x}) - h_i f_i^j(\mathbf{x} - \mathbf{u}_i)). \tag{7}$$

Here we have assumed that all the patterns $\mathbf{f}^j$ are equiprobable *a priori*, but if they were not equiprobable it would be straightforward to include the appropriate probabilities as simple weights in equation (7). Therefore, the recognition of an input pattern consists of first choosing the degradation parameters maximizing the probability in eqution (7) for every pattern in the alphabet, and then choosing the pattern with the largest probability, which will give us the global maximum of the posterior probability distribution. Such maximization can be done separately for each channel, and then multiplying the maximum probability values afterwards. For channel i, and assuming white Gaussian noise, the maximization of the probability is equivalent to the minimization of the following error function:

$$E_i^j = \sum_{\mathbf{x}} (o_i(\mathbf{x}) - h_i f_i^j(\mathbf{x} - \mathbf{u}_i))^2. \tag{8}$$

To minimize this error function we first expand the square of the error function as follows:

$$E_i^j = \sum_{\mathbf{x}} (o_i(\mathbf{x}))^2 + (h_i)^2 \sum_{\mathbf{x}} (f_i^j(\mathbf{x}))^2 - 2h_i \sum_{\mathbf{x}} o_i(\mathbf{x}) f_i^j(\mathbf{x} - \mathbf{u}_i), \tag{9}$$

and then we take partial derivatives with respect to the parameters and equate to zero:

$$\frac{\partial E_i^j}{\partial h_i} = 2h_i K_i^j - 2 \sum_{\mathbf{x}} o_i(\mathbf{x}) f_i^j(\mathbf{x} - \mathbf{u}_i) = 0 \tag{10a}$$

$$\frac{\partial E_i^j}{\partial \mathbf{u}_i} = 2h_i \sum_{\mathbf{x}} o_i(\mathbf{x}) \frac{\partial f_i^j(\mathbf{x} - \mathbf{u}_i)}{\partial \mathbf{u}_i} = 0 \tag{10b}$$

where $K_i^j = \sum_{\mathbf{x}} (f_i^j(\mathbf{x}))^2$. The second condition (equation (10*b*)) is independent of h_i, and it is exactly the same condition that follows from maximizing the traditional correlation function, $\mathrm{corr}_i^j(\mathbf{u}_i) = \sum_{\mathbf{x}} o_i(\mathbf{x}) f_i^j(\mathbf{x} - \mathbf{u}_i)$. Therefore, once we find the $\hat{\mathbf{u}}_i^j$ maximizing the correlation, it follows from equation (10*a*) that $\hat{h}_i^j = \mathrm{corr}_i^j(\hat{\mathbf{u}}_i^j)/K_i^j$. This leads to the following maximum value of the posterior probability for pattern j:

$$P_j = \max\{p(\mathbf{f} = \mathbf{f}^j, \{h_i, \mathbf{u}_i\}|\{\mathbf{o}_i\})\} \propto \exp\left(\frac{1}{2\sigma^2} \sum_{i=1}^{N_c} \hat{h}_i^j \mathrm{corr}_i^j(\hat{\mathbf{u}}_i^j)\right). \tag{11}$$

The correlation operators can be implemented efficiently, as usual in the Fourier domain. The output of this recognition procedure is a set of probabilities independent of the variance of the noise σ^2, assigned to each pattern, from which we select the pattern j with the largest P_j.

3. Implementation and numerical experiments

To test the model, we have conducted a realistic computer simulation, in which the scenario consists of the problem of identification of different species of eagles and falcons, viewed through atmospheric turbulence, with added defocus and noise. The outputs of these simulations are the input blurred images used to test the proposed method, as shown in figure 1. Other previous methods have also been implemented for comparison purposes, as explained next.

3.1. Pattern recognition methods

3.1.1. Bayesian. To implement the Bayesian method, one has to choose the subband decomposition. We have used an efficient implementation of a Gabor multiscale/multiorientation pyramid. The parameters of the Gabor filter bank have been chosen to provide a good sampling of the Fourier domain while maintaining computational efficiency, and are the following.

- Bandwidth (measured along the radial direction) of 1 octave.
- Form factor of unity (isotropic Gaussian envelope).
- Four scales distributed in octaves.
- Highest radial tuning frequency of 1/4 cycles/sample.
- Four principal orientations (0°, 45°, 90° and 135°).

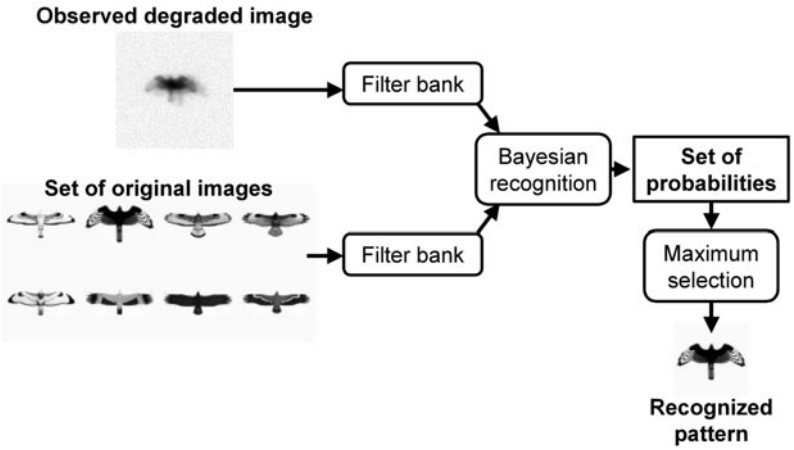

Figure 1. Schematic block diagram of the Bayesian pattern recognition method. A filter bank is applied to both the set of patterns and to the input degraded image. Then the Bayesian method gives the probabilities that the input image corresponds to the different pattern. The output response is the pattern with maximum probability.

With these parameters it is possible to implement the filter bank very efficiently in the spatial domain, using separable convolutions and a pyramidal strategy to obtain the coarser scales.

The Bayesian method consists of computing the MAP for each subband, using the classical method of computing the cross-correlation between the input image and every possible object or pattern. Using equation (11), it follows that the probability that object j generated the observed image is the exponential of a linear combination of the correlation peaks, weighted by the modulus of the OTF for each subband h_i. These OTF values are estimated using conditions in equation (10), as explained above.

3.1.2. Matched filter and POF. As a primary reference, we have implemented the classical method of matched filtering, based on computing the correlation peak between the input scene and each of the possible objects. In the figures and tables, we have labelled this method as 'correlation'.

Alternatively, we have implemented the phase-only filter (POF). It is usual to implement the cross-correlation in the Fourier domain, applying the convolution theorem. This method consists of substituting the Fourier modulus of the cross-correlation by a constant (flat) one. This has several advantages, including an improvement of the results in the presence of optical degradations. In fact, the POF method would be invariant to optical degradations that do not produce phase distortions.

3.1.3. Subband decomposition methods. We have also implemented the previous subband decomposition method proposed by Vargas *et al* [13]. Nevertheless, we have implemented two different versions of it. Version one consisted of reproducing exactly that method, which used a multiscale Laplacian pyramid subband decomposition. The Laplacian pyramid only produces frequency, not orientation subbands, so that it is multiscale, but not multiorientation. We have labelled this version of the method as 'Laplacian'. For a more direct comparison with our Bayesian approach, we have also implemented a second version of the subband decomposition method, simply replacing the Laplacian by the same Gabor pyramid as used in the Bayesian method. We use the label *Gabor* for the resulting method. These two different versions could show a rather different performance, because in the subband method the combination of subbands consists of computing the product of correlation [13], so that if we have a significantly higher number of subbands, such as in the Gabor case, this could strongly affect the performance.

Therefore, we have implemented five different methods: Bayesian, correlation, POF, Laplacian and Gabor.

3.2. Simulation of atmospheric turbulence

A realistic simulation has been implemented, where the objects are different types of flying eagle and falcon (see figure 2(a)). The birds are highly similar in size and overall shape, but exhibit differences mainly in the patterns formed by the feathers, tail or wing shape, and other details. Thus, the discrimination and identification of each species is not straightforward even in optimal viewing conditions. These objects are viewed through a telescope from the ground in the presence of random aberrations induced by atmospheric turbulence. We have considered short-exposure or instantaneous images, in the sense that each image corresponds to a single realization of the random fluctuations. Here, the Zernike coefficients describing the atmospheric optical aberrations are computed based on the classic Kolmogorov model [18]. In particular, the data used here were kindly provided by Cagigal and Canales from the University of Cantabria (Spain), who used their own simulation tool [19]. The statistics of the aberrations is determined by the parameter D/r_0, where D is the pupil diameter of the telescope and r_0 is the Fried parameter, or atmospheric correlation length. As a simplification, we have considered monochromatic light, with wavelength 550 nm. The scale of the different species has been equalized so that the wingspan is about 1 m, and we have considered two viewing distances, of about 90 m, and 180 m. These viewing distances produce images with different scales. In the figures, we refer by 100% scale to the case of 90 m viewing distance, and 50% to the 180 m case, respectively. The scale of the PSF has been adjusted to match these sizes,

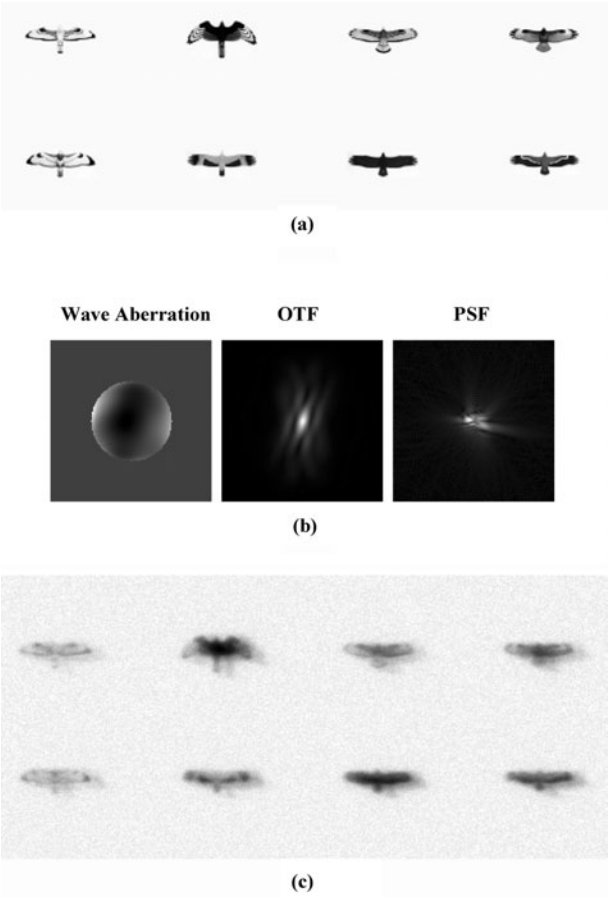

Figure 2. Realistic computer simulation: (a) the set of patterns considered. They correspond to different eagle species. (b) One realization of the optical degradation. The wave aberration (left) has random (turbulence) and deterministic (defocus) parts. The corresponding OTF and PSF are also shown. (c) Degraded images obtained by filtering each pattern with the OTF and adding random noise.

Table 1. Summary of all the conditions considered in the simulations.

Objects (eagles and falcons)	8					
Number of random realizations of turbulence	10					
D/r_0	1	2	4			
Defocus (λ units)	0	λ/4	λ/2	λ	3λ/2	2λ
SNR	20	10	1			
Viewing distance (m)	90	180				

considering $D = 20$ cm. In addition to turbulence, different defocus and additive noise conditions have been simulated, as shown in table 1. Each image is simulated by first computing the OTF from the Zernike coefficients (wave aberration) of the atmospheric turbulence, plus an added amount of defocus. The input object is introduced as a 128 × 128 pixel image (see figure 2), and is filtered by the simulated OTF, and finally three different levels of random Gaussian noise are added to the filtered image.

The complete set of conditions is summarized in table 1. Thus, the total number of images generated in the simulation is 8 (birds) ×10 (random realizations) ×3(D/r_0) × 6 (defocus level) ×3 (SNR) ×2 (distance) = 8640. This large number of images permits us to perform some statistics on the behaviour of the five different methods. Figure 2(c) shows a typical realization of observed images where the degradation suffered by the original images is manifest, so that the recognition is not easy even for a human observer. The conditions of this particular example are $D/r_0 = 2$, defocus = λ/2, SNR = 1, full 100% size (90 m viewing distance).

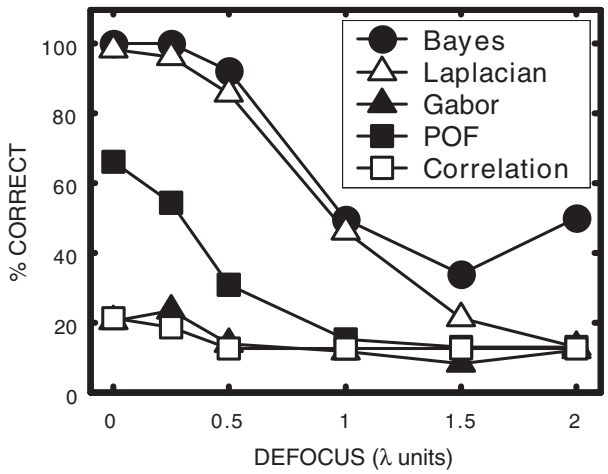

Figure 3. Percentage of correct responses as a function of defocus for the five methods compared: Bayesian (black circles), Laplacian (open triangles), Gabor (black triangles), POF (black squares) and standard correlation (open squares).

4. Results

Figure 3 compares the global averages of the percentage of correct responses provided by the different methods as a function of defocus. In this case, only the highest SNR = 20 has been considered. If we take into account that for defocus = 0 only the atmospheric turbulence is degrading the image, it is clear that only the Bayesian and the Laplacian pyramid methods show a high tolerance to this type of degradation. The correlation and Gabor methods provide poor results just above chance levels (chance level = 12.5%), whereas the POF provides about 60% correct responses. This percentage of the POF method mainly reflects an unequal behaviour: a high rate of correct answers for the easier conditions (low turbulence, and 100% scale) and a poor rate for the more difficult ones (high turbulence and 50% scale), where the POF performance drops rapidly. Regarding the evolution of the curves with defocus, there is a small but important difference between the two best methods. The Bayesian method ensures the 100% correct responses, even in the presence of small amount of defocus (λ/4). The Laplacian method goes basically parallel, just below the Bayesian one, but reaches the chance level for the maximum defocus (2λ). In contrast, the Bayesian method does not decay to chance level even for this high defocus.

Figure 4 compares the percentage of correct responses for three of the conditions tested. The first case corresponds to the best or easiest condition (scale = 100%, defocus = 0, SNR = 20); the second is a difficult condition, with far distance and a very low SNR, but a moderately low defocus (scale = 50%; defocus = λ/2, SNR = 1); the third condition corresponds to a more serious defocus, with full

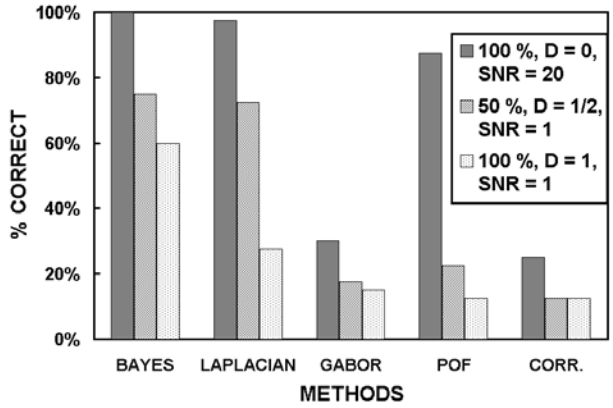

Figure 4. Comparison of the performance of the methods for three particular conditions: scale = 100%, defocus = 0 and SNR = 20 (dark); scale = 50%, defocus = $\lambda/2$ and SNR = 1 (grey); scale = 100%, defocus = λ and SNR = 1 (light grey).

Table 2. Global average of the results obtained for each of the different methods tested.

Methods	Bayesian	Laplacian	Gabor	POF	Correlation
Global percentage correct	71	60	15	33	15

scale of the object and the same very low SNR (scale = 100%; defocus = λ, SNR = 1). The Bayesian method always provides percentage of correct responses above 60% (and equals 100% for zero defocus). The Laplacian method shows a high performance for small amounts of defocus, just below the Bayesian one, but drops for important defocus amounts. The POF does a good job when there is no defocus and the SNR is high, but it hardly tolerates the combined effect of defocus and noise. Again the Gabor and correlation methods perform poorly.

The global percentage correct responses for the complete set of conditions and realizations are listed in table 2 for each method. The Bayesian method clearly performs better than the other methods. This was true for all conditions tested except for scale = 50%, and defocus = λ, where the product of correlations of Laplacian channels was slightly superior. The average result obtained with the proposed Bayesian method confirms this (71% of correct responses, in contrast to the 60% correct provided by the product of Laplacian correlations). Apart from these two methods, both the product of Gabor correlations, and the standard correlation methods, only reached 15% of correct responses, that is a rather poor performance just above chance level (12.5%). Only the POF performed clearly above chance level, providing 33% correct answers, but far from the two first methods.

5. Conclusions

We have presented a novel Bayesian method for pattern recognition in images degraded by unknown general optical degradations and additive noise. The results presented here show that the proposed method is highly robust against optical degradation and noise in the observed image. Our results are consistent with previous works in the sense that the standard correlation, or matched filter method, hardly supports optical degradations. The POF method is much more robust against optical degradations, but it fails when the optical aberrations induce phase distortions in the OTF. The method by Vargas *et al* [13], based on the product of correlations of the Laplacian pyramid decomposition, performs much better than those previous methods, but worse than the proposed Bayesian method, especially for large degradations. The Bayesian method is able to produce reasonable results for the broad class of conditions tested. The coarse approximation introduced for the optical degradation can be interpreted as a regularization that gives a well conditioned problem from the ill conditioned problem that would try to estimate the full OTF of the degradation from the observed image. The method will fail if the OTF changes rapidly or abruptly. In this case, we would need to increase the number of channels to sample more finely the Fourier domain, but there is a trade-off between sampling finely the Fourier domain and regularizing the ill posed problem. The main advantage is its generic degradation model, which is not restricted to defocus, and that includes naturally the noise in the Bayesian framework. Finally, because the method is Bayesian it can be easily adapted to introduce priors on the parameters of the coarse approximation of the degradation's OTF, as well as on the relative abundance of each pattern. Moreover, we can also introduce different costs or penalties when the method fails to recognize the different patterns, which provides a great flexibility for specific applications.

Acknowledgments

This research was partly supported by the Comisón Interministerial de Ciencia y Tecnología under grant DPI2002-04370-C02-02. We want to thank Manuel P Cagigal and Vidal F Canales who kindly provided us atmospheric turbulence aberration data.

References

[1] Javidi B (ed) 2002 *Image Recognition and Classification: Algorithms, Systems, and Applications* (New York: Dekker)
[2] Chan F, Towghi N, Pan L and Javidi B 2000 Distortion tolerant minimum mean squared error filter for detecting noisy targets in environmental degradations *J. Opt. Eng.* **39** 2092–100
[3] Casasent D and Psaltis D 1976 Scale invariant optical correlation using Mellin transforms *Opt. Commun.* **17** 59–63
[4] Hsu Y N and Arsenault H H 1982 Optical pattern recognition using circular harmonic expansion *Appl. Opt.* **21** 4016–9
[5] Gualdron O and Arsenault H H 1994 Improved invariant pattern recognition methods *Real Time Optical Information Processing* ed B Javidi and J Horner (San Diego, CA: Academic) pp 89–113
[6] Fazlolahi A and Javidi B 1997 Error probability of an optimum receiver designed for pattern recognition with nonoverlapping target and scene noise *J. Opt. Soc. Am.* A **14** 1024–32
[7] Towghi N, Javidi B and Li J 1998 Generalized optimum receiver for pattern recognition with multiplicative, additive, and nonoverlapping noise *J. Opt. Soc. Am.* A **15** 1557–65
[8] Vijaya Kumar B V K 1992 Tutorial survey of correlation filters for optical pattern recognition *Appl. Opt.* **31** 4773–801

[9] Refregier P 1999 Bayesian theory for target location in noise with unknown spectral density *J. Opt. Soc. Am.* A **16** 276–83

[10] Towghi N and Javidi B 2001 Optimum receivers for pattern recognition in the presence of Gaussian noise with unknown statistics *J. Opt. Soc. Am.* A **18** 1844–52

[11] Bosch S, Campos J, Montes-Usategui M and Sallent J 1996 Design of correlation filters invariant to degradations characterizable by an optical transfer function *Opt. Commun.* **129** 337–43

[12] Carnicer A, Vallmitjana S, de F Moneo J R and Juvells I 1996 Implementation of an algorithm for detecting patterns in defocused scenes using binary joint transform correlation *Opt. Commun.* **130** 327–36

[13] Vargas A, Campos J and Navarro R 2000 Invariant pattern recognition against defocus based on subband decomposition of the filter *Opt. Commun.* **185** 33–40

[14] Burt O J and Adelson F H 1983 The Laplacian pyramid as a compact image code *IEEE Trans. Commun.* **31** 532–40

[15] Navarro R and Tabernero A 1991 Gaussian wavelet transform: two alternative fast implementations for images *Multidimen. Syst. Signal Process.* **2** 421–36

[16] Navarro R, Tabernero A and Cristobal G 1996 Image representation with Gabor wavelets and its applications *Advances in Imaging and Electron Physics* ed P W Hawkes (San Diego, CA: Academic) pp 1–84

[17] Nestares O, Navarro R, Portilla J and Tabernero A 1998 Efficient spatial-domain implementation of a multiscale image representation based on Gabor functions *J. Electron. Imaging* **7** 166–73

[18] Noll R J 1976 Zernike polynomials and atmospheric turbulence *J. Opt. Soc. Am.* **66** 207–11

[19] Cagigal M P and Canales V F 2000 Generalized Fried parameter after adaptive optics partial wave-front compensation *J. Opt. Soc. Am.* A **17** 903–10